NIH Public Access
Author Manuscript
Circulation. Author manuscript; available in PMC 2006 May 29.

Published in final edited form as:
Circulation. 2005 November 29; 112(22): 3451–3461.

Mitochondrial Dysfunction and Apoptosis Underlie the Pathogenic Process in Alpha-B-Crystallin Desmin Related Cardiomyopathy

Alina Maloyan, PhD, **Atsushi Sanbe, PhD**, **Hanna Osinska, PhD**, **Margaret Westfall, PhD**, **Dustin Robinson, MS**, **Ken-ichi Imahashi, PhD**, **Elizabeth Murphy, PhD**, and **Jeffrey Robbins, PhD**

From the Division of Molecular Cardiovascular Biology, Cincinnati Children's Hospital (A.M., A.S., H.O., J.R.), University of Michigan, Cardiac Surgery Section (M.W., D.R.), Laboratory of Signal Transduction, National Institutes of Environmental Health Sciences, K.-I.I., E.M.)

Abstract

Background—Mitochondria and sarcomeres have a well-defined architectural relationship that partially depends upon the integrity of the cytoskeletal network. An R120G missense mutation in the small heat shock protein alpha-B-crystallin (CryAB) causes desmin-related cardiomyopathy (DRM). DRM is characterized by the formation of intracellular aggregates containing CryAB and desmin that are amyloid positive, and disease can be recapitulated in transgenic mice by cardiac-specific expression of the mutant protein.

Methods and Results—To understand the resultant pathology, we explored the acute effects of R120G expression both in vitro and in vivo. In vitro, transfection of adult cardiomyocytes with R120G-expressing adenovirus resulted in altered contractile mechanics. In vivo, as the cytoskeletal network is disturbed but before deficits in organ function can be detected, alterations in mitochondrial organization and architecture occur, leading to a reduction in the maximal rate of oxygen consumption with substrates that utilize complex I activity, alterations in the Permeability Transition Pore and compromised inner membrane potential. Apoptotic pathways are subsequently activated, which eventually result in cardiomyocyte death, dilation and heart failure.

Conclusions—Cardiac chaperone dysfunction acutely leads to altered cardiomyocyte mechanics, perturbations in mitochondrial-sarcomere architecture and deficits in mitochondrial function, which can result in activation of apoptosis and heart failure.

Keywords

cardiomyopathy; heart diseases; heart failure; molecular biology

Correspondence to: Jeffrey Robbins, Division of Molecular Cardiovascular Biology, 3333 Burnet Avenue, Cincinnati, OH 45229-3039. Tel.: 513-636-8098; Fax: 513-636-3852; email:jeff.robbins@cchmc.org.

Sources of Support: National Institutes of Health Grants HL69799, HL60546, HL52318, HL60546, HL56370 (J.R.) American Heart Association Fellowship (A.M.)

Conflict of Interest Disclosures None. This is an un-copyedited author manuscript that was accepted for publication in Circulation, copyright The American Heart Association. This may not be duplicated or reproduced, other than for personal use or within the "Fair Use of Copyrighted Materials" (section 107, title 17, U.S. Code) without prior permission of the copyright owner, The American Heart Association. The final copyedited article, which is the version of record, can be found at http://circ.ahajournals.org/. The American Heart Association disclaims any responsibility or liability for errors or omissions in this version of the manuscript or in any version derived from it by the National Institutes of Health or other parties.

NIH-PA Author Manuscript
NIH-PA Author Manuscript
NIH-PA Author Manuscript

NIH-PA Author Manuscript
NIH-PA Author Manuscript
NIH-PA Author Manuscript

Introduction

Mutations in desmin, alpha-B-crystallin (CryAB) and other genes result in the desmin-related myopathies (DRM).[1,2] The desminopathies are characterized by accumulations of electron-dense granulofilamentous aggregates in the skeletal and cardiac myocytes. These amorphous bodies contain desmin, CryAB and other proteins that may or may not be shared across the diverse etiologies. Patients normally have distal weakness in their limbs and often show cardiac hypertrophy, conduction block and arrhythmias.[3] Although the initial focus centered on mutations in the intermediate filament protein desmin, it has became apparent that mutations in other proteins that interact with desmin, such as the R120G mutation in CryAB ($CryAB^{R120G}$), can phenocopy the disease.[4] We recently modeled $CryAB^{R120G}$ cardiomyopathy in the mouse by cardiac-specific transgenic (Tg) expression and showed that $CryAB^{R120G}$ expression causes heart failure by 5–7 months.[5]

CryAB is a member of the small heat shock protein family and although it was originally classified as a lens protein, CryAB is present at high concentrations in both cardiac and skeletal muscle and in lower concentrations in brain, skin and kidney. CryAB has chaperone-like, anti-aggregation properties, binds to both desmin and cytoplasmic actin and helps to maintain cytoskeletal integrity. As is the case for other chaperones and the small heat shock proteins, CryAB can bind to unfolded proteins and prevent their denaturation and aggregation. During ischemia, CryAB also binds to the contractile apparatus, presumably protecting the components from denaturation.[6]

Although the genetic etiologies for the DRM's have now been partially defined, the pathogenic sequelae remain obscure, particularly for the $CryAB^{R120G}$-based pathology. The mouse model revealed a collapse of the desmin network and this undoubtedly contributes to the developing disease, yet similar structural changes in the cardiomyocyte's cytoskeleton in another DRM animal model, which expressed a desmin mutation, resulted in significantly less morbidity and no mortality.[7] Therefore it seems likely that expression of mutant CryAB has other effects, in addition to leading to alterations in the desmin network, and indeed we noted that aggregates in the $CryAB^{R120G}$ cardiomyocytes invariably contain amyloid-like material while those in the desmin mutant cells do not.[8]

In comparing the two models, $CryAB^{R120G}$ cardiomyocyte mitochondrial organization and architecture appeared to be disproportionately affected in the young adults (unpublished data). Mitochondrial organization is rigidly controlled in both skeletal and cardiac myocytes and depends upon the integrity of the cytoskeleton.[9] To explore whether early pathological processes involved mitochondrial dysfunction and to determine the pathogenic basis for the heart failure observed in the $CryAB^{R120G}$ mice, we have now defined the acute and chronic effects of cardiomyocyte $CryAB^{R120G}$ expression in vitro and in vivo. $CryAB^{R120G}$ expression quickly leads to visible aggregates and their accumulation results in deficits in contractile behavior as the cell contracts at high rates. These acute effects are rapidly followed by alterations in mitochondrial-sarcomere architecture and function, which eventually lead to activation of apoptotic pathways that further compromise cardiomyocyte function and viability, resulting in the development of heart failure and death.

Methods

Transgenic Mice

FVB/N mice with cardiac-specific overexpression of normal CryAB (wild type) or CryAB containing the R120G missense mutation ($CryAB^{R120G}$), driven by the α-myosin heavy chain promoter have been described.[5] Transgenic mice were identified by PCR analysis of DNA isolated from tail clips.

NIH-PA Author Manuscript

NIH-PA Author Manuscript

NIH-PA Author Manuscript

Antibodies

Anti-Caspase-3 antibody and anti-VDAC were obtained from Calbiochem and anti-activated caspase-3 from Abcam, Inc. Anti-cytochrome *c* was purchased from BD Biosciences and anti-cTnI antibody (MAB1691) from Chemicon.

An expanded Methods section is included as Online Supplemental Material.

Results

CryAB^{R120G} Expression Affects Cardiomyocyte Contractility

We wished to determine whether CryAB^{R120G} expression had acute effects on cardiomyocyte mechanics. Changes in cardiomyocyte contractility can be caused by altered sarcomeric function, modifications in passive cytoskeletal stiffness, or structural changes in sarcomere organization. In order to understand the acute effects of CryAB^{R120G} on contractility, isolated adult cardiomyocytes were transfected with adenoviruses carrying CryAB^{R120G} or wild type (WT) CryAB. In preliminary experiments, we found that a multiplicity of infection of 100 yielded a level of overexpression that approximated that observed in the CryAB^{R120G} mice previously reported;[5] when quantitated, protein accumulations did not differ significantly between the CryAB^{R120G} and CryAB^{WT} cultures (Figure 1A). The cells tolerated significant levels of CryAB expression, with both the overall morphology and integrity of the contractile apparatus preserved (Figure 1B), consistent with previous data that confirmed cell integrity and the lack of non-specific structural or functional changes upon adeno-mediated gene transfer.[10,11] Cells transfected with CryAB^{R120G} showed the characteristic punctate pattern of densely staining material consistent with early aggregate formation (Figure 1B). The cells were then paced at either 0.2 or 2 Hz and the magnitude and velocity of shortening and relaxation determined. Strikingly, after only 4 days of CryAB^{R120G} expression, those cardiomyocytes showed marked arrhythmias upon pacing at the faster rate (Figure 1C). Additionally, when paced at 2 Hz, both peak shortening and the maximum departure velocity were significantly less in the CryAB^{R120G} cells (Figure 1C–E). Function in the CryAB^{WT} transfected cells was comparable to control myocytes and confirmed that the effects observed were specific to the mutant protein.

Mitochondrial Alterations Result from CryAB^{R120G} Expression

Intermediate filaments associate with mitochondria in many cell types, including skeletal and cardiac myocytes. In the last decade, using a number of different approaches including loss of function, it has become apparent that the cytoskeleton in general and the intermediate filaments in particular play an important role in mitochondrial localization and transport.[9,12,13] In our previous analyses of cardiac tissue from CryAB^{R120G} mice, we noted that disruption of the desmin network occurred early in 3 month adults with detectable aggregation of desmin and CryAB.[5] To assess whether mitochondrial ultrastructure was also affected by CryAB^{R120G} expression we examined cardiomyocyte ultrastructure at 6 weeks when the sarcomeric architecture is fully developed (Figure 2). At this time, no functional deficits as analyzed by echocardiography, or histological abnormalities could be detected, nor had any detectable hypertrophy occurred. Although electron microscopy did not show any gross alterations in mitochondrial morphology, the overall architecture of the mitochondrial arrangement with the sarcomeres was significantly altered in the CryAB^{R120G} cardiomyocytes. The normal arrangement, in which the mitochondria are packed between the sarcomeres in a well-ordered array with their transverse boundaries tightly linked to the Z line, was perturbed, with bundles of unaligned mitochondria frequently apparent (Figure 2A). Although there were obvious morphological changes in the gross architecture of the mitochondria, most appeared to be relatively intact, with dense, well-ordered cristae, although mitochondria immediately surrounding nascent aggregates were clearly affected. To ascertain their functional state,

NIH-PA Author Manuscript

NIH-PA Author Manuscript

NIH-PA Author Manuscript

mitochondria were isolated from the nontransgenic (Ntg) and Tg hearts and the maximum rate of ADP stimulated oxygen consumption (V_{max}) with glutamate and malate as substrate determined. Surprisingly, even at this early stage when cardiac disease is not apparent, V_{max} was reduced by ~50% in mitochondria derived from the $CryAB^{R120G}$ hearts (Figure 2B). To identify the site of the defect in respiration, we examined the maximal uncoupler stimulated respiration rate with substrates that enter at different sites along the electron transport chain. Glutamate and malate generate NADH, which enters via the NADH dehydrogenase-complex I site. With glutamate/malate as substrate, the Tg mitochondria exhibited significantly lower rates of uncoupler stimulated oxygen consumption, consistent with the reduced V_{max} for oxygen consumption in the Tg mitochondria. Interestingly, with either succinate or ascorbate + N,N,N′,N′-tetramethyl-p-phenylenediamine (TMPD) as substrate, there was no difference in oxygen consumption between NTg or Tg mitochondria. Succinate enters the electron transport chain via succinate dehydrogenase or complex II. TMPD can donate electrons directly to cytochrome *c*, thereby bypassing complexes I, II and III. These data point to a specific defect in mitochondrial complex I in the $CryAB^{R120G}$ hearts, as substrates that enter downstream of complex I show similar rates of oxygen consumption in the NTg and Tg mitochondria. To examine whether this defect in maximal oxygen respiration was an artifact due to isolation of the mitochondria, we also measured the maximum rate of respiration with glutamate and malate as substrate in saponin permeabilized myocytes (Figure 2B). Consistent with the data obtained from the heart isolations, V_{max} in the permeabilized $CryAB^{R120G}$ myocytes was significantly less when compared to the NTg myocytes.

Opening of the permeability transition pore (PTP) at the inner mitochondrial membrane activates the mitochondrial permeability transition, leading to mitochondrial swelling, depolarization and release of the internal ion pool. The PTP is a multiprotein complex that is formed at the intersection of the outer and inner mitochondrial membranes. The PTP is responsible for membrane permeabilization and is made up of the voltage dependent anion channel (VDAC), the adenine nucleotide translocator and other mitochondrial membrane-associated proteins. PTP opening and mitochondrial swelling is classically determined by challenging isolated mitochondria with Ca^{2+} and measuring the decrease in light scattering. Induced mitochondrial swelling in isolated intact heart mitochondria from NTg mice led to a significant decrease in absorbance (Figure 2C). In contrast, the mitochondria from 2 month old Tg mice were already compromised, as detected by the decrease in the basal absorbance at 540 nm and a less pronounced Ca^{2+} response. To confirm that Ca^{2+}-induced mitochondrial swelling was due to PTP opening, we examined the effects of the PTP inhibitor cyclosporin (CsA). CsA, which was added before the addition of Ca^{2+}, significantly abrogated mitochondrial swelling in mitochondria isolated from 2 month Tg hearts. Further attenuation of the Ca^{2+} response was observed in the hearts from 6 month old $CryAB^{R120G}$ Tg mitochondria.

Despite the lack of obvious pathology at 6–8 weeks, we reasoned that if the mitochondria were truly involved in a primary pathogenic response, this should be manifested at the whole organ level. To that end, ^{31}P-NMR spectra were used to evaluate phosphocreatine (Pcr) levels in 8 week $CryAB^{WT}$ and $CryAB^{R120G}$ Langendorff-perfused hearts (Figure 2D). Decreased Pcr/ATP ratios are a predictor of mortality in patients with cardiomyopathy[14] and we reasoned, based upon the above data, that this ratio would be affected in the mice. Even at this early age, we observed a significant decrease in PCr/ATP in the $CryAB^{R120G}$ hearts (1.60 ± 0.08, $n = 8$) compared to $CryAB^{WT}$ hearts (1.96 ± 0.09, n=8, $P < 0.05$).

Considering the early appearance of mitochondrial dysfunction, we suspected that there might be a direct association of the normal or mutant protein with mitochondria. Cytosolic and mitochondrial fractions were isolated and the protein composition of each determined with respect to CryAB and desmin concentrations. Strikingly, the mitochondrial fraction derived from the $CryAB^{R120G}$ hearts contained a significantly higher percentage of total CryAB

NIH-PA Author Manuscript

NIH-PA Author Manuscript

NIH-PA Author Manuscript

compared to either the NTg or CryAB^{WT}-Tg material, while desmin levels were only modestly higher (Figure 3A). On the basis of the data presented in Figure 2, we suspected a specific interaction of CryAB^{R120G} with components of the PTP and consistent with this hypothesis, immunoprecipitation with VDAC shows a strong interaction with CryAB^{R120G} but almost none with CryAB derived from Ntg or CryAB^{WT} overexpressing hearts (Figure 3B). Western analysis for the presence of desmin in the anti-VDAC-precipitated material confirmed that non-specific contamination with the desmin-positive aggregates, which also contain CryAB, was not responsible for the CryAB-positive signal (Figure 3B). We conclude that CryAB^{R120G} can strongly interact with VDAC in the mice before overt disease presents.

Activation of Apoptosis in CryAB^{R120G} Mice

Mitochondrial permeability transition and swelling can result in cytochrome *c* release and subsequent activation of apoptosis. We measured cytochrome *c* in both the cytosolic and mitochondrial fractions and observed progressive release of cytochrome *c* into the cytoplasm as pathology progressed (Figure 4A). Cytochrome *c* was present exclusively in the mitochondrial fractions of NTg and 2–4 month old CryAB^{R120G} mice. By 6 months, when the Tg mice show acute symptoms of heart failure,[5] cytochrome *c* was observed almost exclusively in the cytosolic compartment. To confirm the activation of apoptotic processes in the CryAB^{R120G} cardiomyocytes, we examined caspase-3 cleavage in the hearts from 5–6 month old NTg and CryAB^{R120G} mice. Confocal microscopy (Figure 4B) and Western analysis (Figure 4C) confirmed high levels of caspase-3 activation in the CryAB^{R120G} hearts during the latter stages of the disease and the absence of any detectable caspase-3 activity in the comparable Ntg hearts. TUNEL assays carried out on 5 month hearts derived from CryAB^{R120G} and CryAB^{WT} mice confirmed the elevated apoptotic indices were due to overexpression of the mutant protein and not simply reflecting a generalized response to high levels of CryAB (Figure 4D and 4E).

CryAB^{R120G} Expression Affects the Mitochondrial Permeability Transition Pore

To confirm that the mitochondrial alterations and activation of cell death pathways could be acutely activated by CryAB^{R120G} overexpression, rat neonatal cardiomyocytes (RNC) were transfected with adenoviruses containing CryAB^{WT} or CryAB^{R120G}. Dissipation of mitochondrial membrane potential ($\Delta\psi$) is a critical event in the process of cell death. To examine whether CryAB^{R120G} overexpression was associated with changes in $\Delta\psi$, we measured the ability of the transfected cells' mitochondria to take up and retain the mitochondrion-selective dye tetra-methyl-rhodamine ester (TMRE). TMRE is a fluorescent probe whose accumulation and subsequent retention is dependent upon $\Delta\psi$, and is used to image time-dependent mitochondrial membrane potential. Figure 5A shows representative histograms and density plots from RNC that were transfected with either CryAB^{WT} or CryAB^{R120G}-containing adenovirus and subjected to FACS analysis. Overexpression of CryAB^{R120G} decreased TMRE fluorescence and shifted the distribution curve leftward, indicating depolarization of $\Delta\psi$, relative to either the control RNC or those transfected with CryAB^{WT}. The summarized data (Figure 5B) show that approximately 90% of non-transfected and 70% of CryAB^{WT}-transfected RNC retained high levels of fluorescence as compared to 9% of the CryAB^{R120G}-transfected cardiomyocytes ($P < 0.0001$ versus Control).

To characterize PTP activation at the single cardiomyocyte level, time-lapse confocal microscopy was performed with TMRE-loaded RNC. Non-transfected, CryAB^{WT}- or CryAB^{R120G}-transfected cardiomyocytes were treated with the mitochondrial uncoupler, CCCP, and time-dependent TMRE loss monitored by time-lapse scanning (Figure 6). Sequential images obtained from individual cells showed the rapid loss of signal from the CryAB^{R120G} transfected cells, relative to those transfected with CryAB^{WT}. CryAB^{R120G} expression not only decreased cardiomyocyte $\Delta\psi$, but also accelerated the onset of TMRE loss,

NIH-PA Author Manuscript

NIH-PA Author Manuscript

NIH-PA Author Manuscript

suggesting that PTP opening had already occurred. CsA treatment of the CryAB^{R120G} RNC confirmed that the rapid loss observed was due to PTP opening (Figure 6B). The calculated time to 50% percent of TMRE loss in CryAB^{R120G}-transfected myocytes was 95 seconds compared to approximately 200 seconds in the non-transfected or CryAB^{WT} transfected cardiomyocytes (Figure 6C).

Considering the effects on mitochondrial morphology, architecture and function, as well as the appearance of apoptotic cells in the CryAB^{R120G} hearts, we examined whether CryAB^{R120G} expression also led to activation of apoptosis in transfected RNC. Apoptotic cell death was clearly present in transfected cardiomyocytes as indicated by the appearance of early (annexin V) mid (caspase-3) and late (TUNEL) apoptotic markers (Figure 7A). Essentially all of the transfected cardiomyocytes stained positively for annexin V and quantitation of caspase-3 showed a 3.5-fold upregulation in CryAB^{R120G}-transfected RNC as compared to non-transfected cardiomyocytes (Figure 7B).

Discussion

DRM is a subgroup of myofibrillar myopathy caused by mutations in desmin, CryAB and other proteins that interact with the intermediate filaments. The pathology is characterized by myofibril disruption that appears to initiate at the Z-disk. Dislocation and aggregation of membranous organelles is observed as well as the accumulation of the mutant, misfolded desmin and/or CryAB into insoluble aggregates, which gradually increase in the cytoplasm and are thought to eventually result in cell death.[1–3] We previously showed that these aggregates may be classified as aggresomes, whose accumulation is often associated with neurodegenerative diseases caused by protein misfolding or unfolding.[8] Our studies showed that the aggresomes present in the cardiomyocytes contain large concentrations of a toxic amyloid oligomer, which is typically found in many of the amyloid-based neurodegenerative diseases. The data thus link these cardiomyopathies to a broad class of amyloid-based neurodegenerative disease and offer potential insight into the mechanistic bases for the cardiac pathology that eventually results in dilation and death by heart failure.[5]

A loss of desmin or CryAB function has been thought to be an underlying cause for the development of cardiomyopathy and heart failure in DRM patients due to either the inability of the mutant desmin to maintain cytoskeletal integrity or by the loss by CryAB's chaperone function, which would subsequently lead to desmin misfolding and eventual formation of the characteristic aggregates. Although loss of function may indeed contribute to the pathology, it cannot explain it completely, as we have noted a relatively benign cardiac phenotype, compared to the CryAB^{R120G} animals, in homozygous CryAB knockout mice (Maloyan and Robbins, unpublished observations). We think it likely that CryAB^{R120G} expression leads to a multi-focal pathology. There appears to be physical and mechanical repercussions of CryAB^{R120G} expression, probably due to the development of the small protein aggregates. Viral transfection into adult rat myocytes, show that the acute effects of CryAB^{R120G} expression result in significant deficits in both peak shortening and maximum departure velocity with irregular contraction when pacing is increased to 2 Hz (Figure 1). In addition to the altered cardiomyocyte mechanics in Figure 1, we showed previously that in transfected cardiomyocytes amyloid oligomer was present within 48–60 hours post-transfection,[8] and in the CryAB^{R120G} mice as soon as 2–3 days after the transgene is activated (Robbins, unpublished data). However, even in the intensely studied neurodegenerative disease processes thought to be due to amyloid oligomer toxicity, the exact sequence of events leading from amyloid formation to cell death is unknown. Several potentially damaging pathways are activated, including oxidative stress and mitochondrial dysfunction.[15–17] Recently, a direct linkage between β-amyloid and the mitochondria was defined, with β-amyloid binding to the mitochondrial protein Aβ alcohol dehydrogenase.[18]

NIH-PA Author Manuscript

NIH-PA Author Manuscript

NIH-PA Author Manuscript

The data in this study further underscore the parallels between CryAB^{R120G} cardiomyopathy and the amyloid-based neurodegenerative pathologies, as mitochondrial dysfunction appears to be an early event in the cardiac pathology, appearing by 6–8 weeks and before any overt changes in organ function can be detected. The biochemical, functional and structural alterations resulted in a significantly compromised Pcr/ATP ratio in early adulthood (Figure 2) before overt functional deficits present. A number of processes could lead to early involvement of the mitochondria. Mitochondria are held in position and can be transported in the cytoplasm through their interactions with cytoskeletal components such as the microtubules and intermediate filaments.[19] We have noted that disruption of the desmin network rapidly leads to alterations in mitochondrial positioning and structure,[5] and similar observations have been made in striated muscle derived from the desmin knockout mice, with severe mitochondrial deficits presenting in both heart and skeletal muscle.[9,13] We hypothesize that disturbance of the tight juxtaposition of the mitochondria over the interior of the sarcomere results in alterations in cellular metabolism. Our data are consistent with CryAB^{R120G} specifically associating with mitochondria through VDAC interaction early in the pathogenic process. The significance of the preferential association of CryAB^{R120G} versus the normal protein with VDAC is unclear but raises the possibility that CryAB^{R120G} may have a direct impact on either VDAC or a mitochondrial protein associated with the PTP. What is clear is that mitochondrial dysfunction is one of the earliest detectable events in the development of R120G-mediated cardiomyopathy and appears to play a major role in the developing pathology. As early as 6 weeks there is a significant reduction in complex I activity and mitochondrial respiration is significantly compromised. Mitochondrial permeability transition is clearly affected in CryAB^{R120G} transfected cardiomyocytes and precedes the increased levels of apoptotic markers.

The connections between amyloid deposition, mitochondrial dysfunction and cell degeneration and death remain contentious. However, there are increasing data linking amyloidogenic proteins to mitochondrial toxicity. The exposure of isolated brain mitochondria to β-amyloid causes a decrease in mitochondrial enzyme activity, respiration and membrane potential.[20] β-amyloid can activate PTP opening, resulting in mitochondrial swelling,[21] a result consistent with our observations. Impaired function of complex I has also been linked to the development of Parkinson's and Alzheimer's diseases,[17,22,23] and in Down's syndrome there are reduced levels of complex I in the cerebellum.[24] In Parkinson's disease, the proteins parkin and α-synuclein, which are components of the abnormal aggregates (Lewy bodies) found in patient neurons, bind to one another in vitro and inhibition of the mitochondrial respiratory chain will increase incorporation of α-synuclein into the aggregates in vitro.[25] Finally, deficits in energy metabolism have been proposed as a primary pathogenic mechanism in Huntington's disease, with elevated lactate levels being detected in the occipital cortex and basal ganglia.[26] Ultrastructural analyses have demonstrated that mutant huntingtin appears to be present on neuronal mitochondrial membranes[27] and can directly increase mitochondrial susceptibility to calcium-induced permeability transition, resulting in the release of cytochrome *c*.[28] These studies are consistent with the mechanisms that might be involved in CryAB^{R120G} pathogenesis, as our data show that CryAB^{R120G} expression leads to detectable amyloid formation in the cardiomyocytes[8] and mitochondrial dysfunction, which, in turn, could contribute to a more rapid amyloid accumulation and an inherently unstable feed-forward loop.

The release of cytochrome *c* is a well-defined mechanism for activation of apoptosis and, in the last few years, the potential importance of apoptosis in heart failure has been defined.[29–32] Wencker established a causal role by showing that very low levels of myocyte apoptosis were sufficient to cause a lethal, dilated cardiomyopathy.[31] In a retrospective study on 33 patients who had died of acute myocarditis, cardiomyocyte apoptosis was identified as a common mechanism of myocardial damage with significantly more apoptotic cardiomyocytes present in patients who had died from progressive heart failure compared with those who died

NIH-PA Author Manuscript

NIH-PA Author Manuscript

NIH-PA Author Manuscript

suddenly from cardiac arrest.[33] Cardiomyocytes transfected with CryAB^{R120G} show striking activation of both early and late apoptotic markers, confirming the potential of an acute response upon mutant CryAB expression. Significantly, we also found high levels of activated caspase-3 in the CryAB^{R120G} Tg hearts in the later disease stages of progressive heart failure (Figure 4). Taking into consideration that the progression of cardiomyopathy and heart failure in CryAB^{R120G} mice occurs over a 5–7 month period, our model underscores the potential importance of apoptosis in progressive heart failure.

Our data point to the importance of a progressive pathology in the development of heart failure. It is clear that expression of CryAB^{R120G} has acute effects on cardiomyocyte mechanics, affecting contractility through as yet undefined mechanisms, although the accumulating aggregates could certainly play a physical role in attenuating normal cardiomyocyte contractile behavior. Alterations in contractility can be sensed by multiple mechanisms, resulting in global responses at the transcriptional and translational levels but we believe that a crucial aspect of the early pathology is linked to alterations in respiration. Mitochondria-sarcomere architecture is affected very early and complex I activity is significantly attenuated with reductions of 50% by 6 weeks, before alterations in cardiac function can be detected. This is rapidly followed by compromised PTP function and mitochondrial swelling. These become more severe over a period of 2–3 months, eventually leading to release of cytochrome *c* and activation of apoptosis.

Supplementary Material

Refer to Web version on PubMed Central for supplementary material.

Acknowledgements

This work was supported by National Institutes of Health grants HL69779, HL56370, HL074728, HH61638 and HL52318 (J.R.) and by a American Heart Association Fellowship (A.M.).

References

1. Engel AG. Myofibrillar myopathy. Ann Neurol 1999;46:681–683. [PubMed: 10553983]
2. Paulin D, Huet A, Khanamyrian L, Xue Z. Desminopathies in muscle disease. J Pathol 2004;204:418–427. [PubMed: 15495235]
3. Goldfarb LG, Vicart P, Goebel HH, Dalakas MC. Desmin myopathy. Brain 2004;127:723–734. [PubMed: 14724127]
4. Vicart P, Caron A, Guicheney P, Li Z, Prevost MC, Faure A, Chateau D, Chapon F, Tome F, Dupret JM, Paulin D, Fardeau M. A missense mutation in the alphaB-crystallin chaperone gene causes a desmin-related myopathy. Nat Genet 1998;20:92–95. [PubMed: 9731540]
5. Wang X, Osinska H, Klevitsky R, Gerdes AM, Nieman M, Lorenz J, Hewett T, Robbins J. Expression of R120G-alphaB-crystallin causes aberrant desmin and alphaB-crystallin aggregation and cardiomyopathy in mice. Circ Res 2001;89:84–91. [PubMed: 11440982]
6. Golenhofen N, Htun P, Ness W, Koob R, Schaper W, Drenckhahn D. Binding of the stress protein alpha B-crystallin to cardiac myofibrils correlates with the degree of myocardial damage during ischemia/reperfusion in vivo. J Mol Cell Cardiol 1999;31:569–580. [PubMed: 10198188]
7. Wang X, Osinska H, Dorn GW 2nd, Nieman M, Lorenz JN, Gerdes AM, Witt S, Kimball T, Gulick J, Robbins J. Mouse model of desmin-related cardiomyopathy. Circulation 2001;103:2402–2407. [PubMed: 11352891]
8. Sanbe A, Osinska H, Saffitz JE, Glabe CG, Kayed R, Maloyan A, Robbins J. Desmin-related cardiomyopathy in transgenic mice: a cardiac amyloidosis. Proc Natl Acad Sci U S A 2004;101:10132–10136. [PubMed: 15220483]
9. Reimann J, Kunz WS, Vielhaber S, Kappes-Horn K, Schroder R. Mitochondrial dysfunction in myofibrillar myopathy. Neuropathol Appl Neurobiol 2003;29:45–51. [PubMed: 12581339]
10. Westfall MV. Myofilament protein phosphorylation by PKC in genetically engineered adult cardiac myocytes. Methods Mol Biol 2003;219:159–166. [PubMed: 12597006]

NIH-PA Author Manuscript

NIH-PA Author Manuscript

NIH-PA Author Manuscript

11. Westfall MV, Borton AR. Role of troponin I phosphorylation in protein kinase C-mediated enhanced contractile performance of rat myocytes. J Biol Chem 2003;278:33694–33700. [PubMed: 12815045]
12. Capetanaki Y. Desmin cytoskeleton: a potential regulator of muscle mitochondrial behavior and function. Trends Cardiovasc Med 2002;12:339–348. [PubMed: 12536120]
13. Linden M, Li Z, Paulin D, Gotow T, Leterrier JF. Effects of desmin gene knockout on mice heart mitochondria. J Bioenerg Biomembr 2001;33:333–341. [PubMed: 11710808]
14. Neubauer S, Horn M, Cramer M, Harre K, Newell JB, Peters W, Pabst T, Ertl G, Hahn D, Ingwall JS, Kochsiek K. Myocardial phosphocreatine-to-ATP ratio is a predictor of mortality in patients with dilated cardiomyopathy. Circulation 1997;96:2190–2196. [PubMed: 9337189]
15. Andersen JK. Oxidative stress in neurodegeneration: cause or consequence? Nat Med 2004;10 (Suppl):S18–25. [PubMed: 15298006]
16. Brown GC, Borutaite V. Inhibition of mitochondrial respiratory complex I by nitric oxide, peroxynitrite and S-nitrosothiols. Biochim Biophys Acta 2004;1658:44–49. [PubMed: 15282173]
17. Jordan J, Cena V, Prehn JH. Mitochondrial control of neuron death and its role in neurodegenerative disorders. J Physiol Biochem 2003;59:129–141. [PubMed: 14649878]
18. Lustbader JW, Cirilli M, Lin C, Xu HW, Takuma K, Wang N, Caspersen C, Chen X, Pollak S, Chaney M, Trinchese F, Liu S, Gunn-Moore F, Lue LF, Walker DG, Kuppusamy P, Zewier ZL, Arancio O, Stern D, Yan SS, Wu H. ABAD directly links Abeta to mitochondrial toxicity in Alzheimer's disease. Science 2004;304:448–452. [PubMed: 15087549]
19. Vendelin M, Beraud N, Guerrero K, Andrienko T, Kuznetsov AV, Olivares J, Kay L, Saks VA. Mitochondrial regular arrangement in muscle cells: a "crystal-like" pattern. Am J Physiol Cell Physiol 2005;288:C757–767. [PubMed: 15496480]
20. Casley CS, Canevari L, Land JM, Clark JB, Sharpe MA. Beta-amyloid inhibits integrated mitochondrial respiration and key enzyme activities. J Neurochem 2002;80:91–100. [PubMed: 11796747]
21. Cardoso SM, Santos S, Swerdlow RH, Oliveira CR. Functional mitochondria are required for amyloid beta-mediated neurotoxicity. Faseb J 2001;15:1439–1441. [PubMed: 11387250]
22. Love R. Mitochondria back in the spotlight in Parkinson's disease. Lancet Neurol 2004;3:326. [PubMed: 15176404]
23. Baloyannis SJ, Costa V, Michmizos D. Mitochondrial alterations in Alzheimer's disease. Am J Alzheimers Dis Other Demen 2004;19:89–93. [PubMed: 15106389]
24. Busciglio J, Pelsman A, Wong C, Pigino G, Yuan M, Mori H, Yankner BA. Altered metabolism of the amyloid beta precursor protein is associated with mitochondrial dysfunction in Down's syndrome. Neuron 2002;33:677–688. [PubMed: 11879646]
25. Lee HJ, Shin SY, Choi C, Lee YH, Lee SJ. Formation and removal of alpha-synuclein aggregates in cells exposed to mitochondrial inhibitors. J Biol Chem 2002;277:5411–5417. [PubMed: 11724769]
26. Jenkins BG, Koroshetz WJ, Beal MF, Rosen BR. Evidence for impairment of energy metabolism in vivo in Huntington's disease using localized 1H NMR spectroscopy. Neurology 1993;43:2689–2695. [PubMed: 8255479]
27. Gutekunst CA, Li SH, Yi H, Ferrante RJ, Li XJ, Hersch SM. The cellular and subcellular localization of huntingtin-associated protein 1 (HAP1): comparison with huntingtin in rat and human. J Neurosci 1998;18:7674–7686. [PubMed: 9742138]
28. Choo YS, Johnson GV, MacDonald M, Detloff PJ, Lesort M. Mutant huntingtin directly increases susceptibility of mitochondria to the calcium-induced permeability transition and cytochrome c release. Hum Mol Genet 2004;13:1407–1420. [PubMed: 15163634]
29. Gustafsson AB, Gottlieb RA. Mechanisms of apoptosis in the heart. J Clin Immunol 2003;23:447–459. [PubMed: 15031632]
30. Regula KM, Kirshenbaum LA. Apoptosis of ventricular myocytes: a means to an end. J Mol Cell Cardiol 2005;38:3–13. [PubMed: 15623417]
31. Wencker D, Chandra M, Nguyen K, Miao W, Garantziotis S, Factor SM, Shirani J, Armstrong RC, Kitsis RN. A mechanistic role for cardiac myocyte apoptosis in heart failure. J Clin Invest 2003;111:1497–1504. [PubMed: 12750399]
32. Foo RS, Mani K, Kitsis RN. Death begets failure in the heart. J Clin Invest 2005;115:565–571. [PubMed: 15765138]

NIH-PA Author Manuscript

NIH-PA Author Manuscript

NIH-PA Author Manuscript

33. Kyto V, Saraste A, Saukko P, Henn V, Pulkki K, Vuorinen T, Voipio-Pulkki LM. Apoptotic cardiomyocyte death in fatal myocarditis. Am J Cardiol 2004;94:746–750. [PubMed: 15374778]

NIH-PA Author Manuscript

NIH-PA Author Manuscript

NIH-PA Author Manuscript

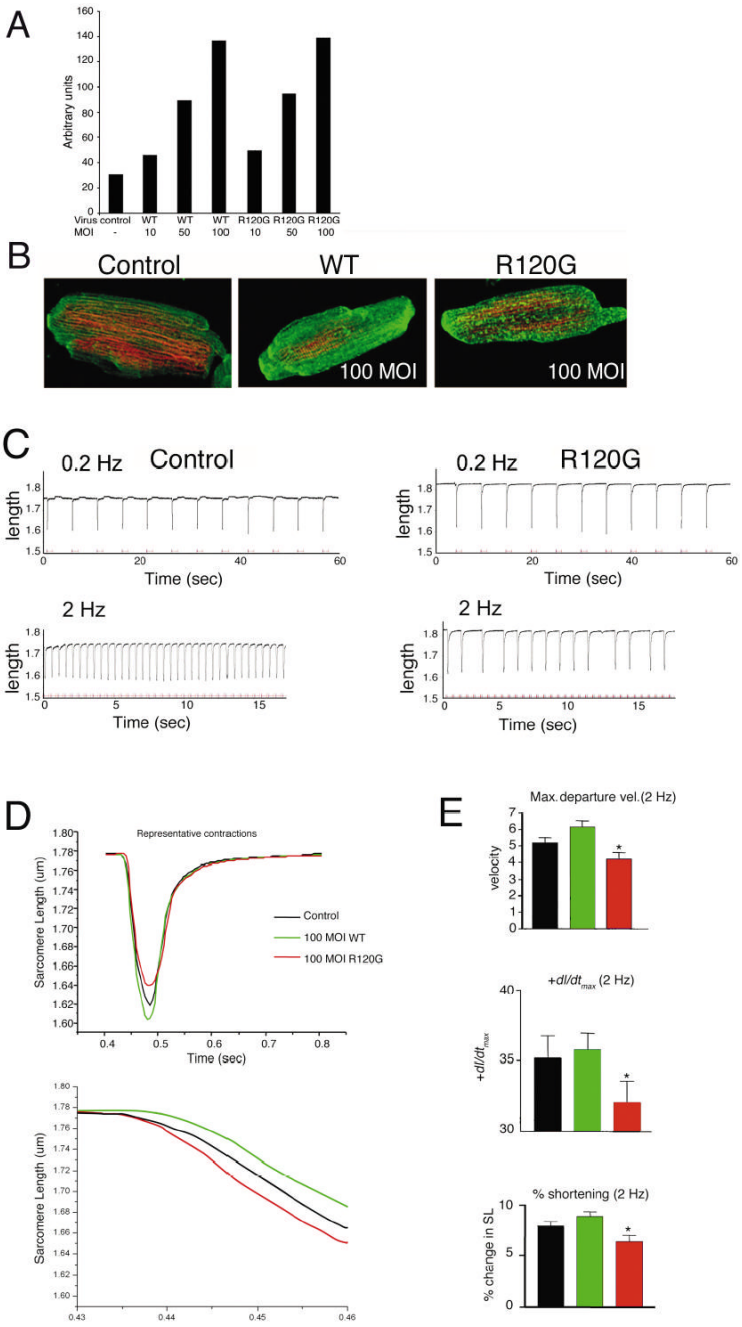

Figure 1.

Contractile function of adult cardiomyocytes transfected with wild type or mutant CryAB. A, Representative histogram of western blots of CryAB^{WT} and CryAB^{R120G} expression in transfected cardiomyocytes as a function of the multiplicity of infection (MOI). MOI's of 100 resulted in protein expression equivalent to that observed in the Tg mouse model of DRM.[5] B, Immunofluorescent images of adult rat cardiomyocytes 5 days post-infection. Conservation of the contractile apparatus is apparent. Control indicates cardiomyocytes that were transfected at the same MOI with vehicle only. C, Representative steady state single recordings of sarcomere shortening obtained in control myocytes (left panel) and myocytes expressing CryAB^{R120G} (right panel) stimulated at 0.2 Hz (60 seconds, upper traces) and 2.0 Hz (~15

NIH-PA Author Manuscript

NIH-PA Author Manuscript

NIH-PA Author Manuscript

seconds, lower traces). Note the inability of myocytes expressing $CryAB^{R120G}$ to maintain pacing at 2.0 Hz. Recordings from myocytes expressing $CryAB^{WT}$ were not significantly different from control recordings. D, Composite sarcomere shortening traces for myocytes from control, $CryAB^{WT}$, and $CryAB^{R120G}$ groups paced at 2 Hz. These traces demonstrate the significant decrease in peak shortening, departure velocity and $+dP/dt_{max}$ for myocytes expressing $CryAB^{R120G}$ as shown in (C). Composite traces for $CryAB^{R120G}$ myocytes do not include stimuli that were not followed by cell shortening. Baseline sarcomere length, departure and return velocity, $\pm dP/dt_{max}$ and peak shortening were not significantly different in myocytes from either the control, $CryAB^{WT}$, or $CryAB^{R120G}$ transfected cells at 0.2 Hz. E, Analysis of contractile shortening in myocytes from control ($n = 39$), $CryAB^{WT}$ (100 MOI, $n = 26$), and $CryAB^{R120G}$ (100 MOI, $n = 29$) groups. Peak shortening, departure velocity and $+dP/dt_{max}$ decreased significantly ($P < 0.05$) in myocytes expressing $CryAB^{R120G}$ compared to control and WT CryAB myocytes.

NIH-PA Author Manuscript
NIH-PA Author Manuscript
NIH-PA Author Manuscript

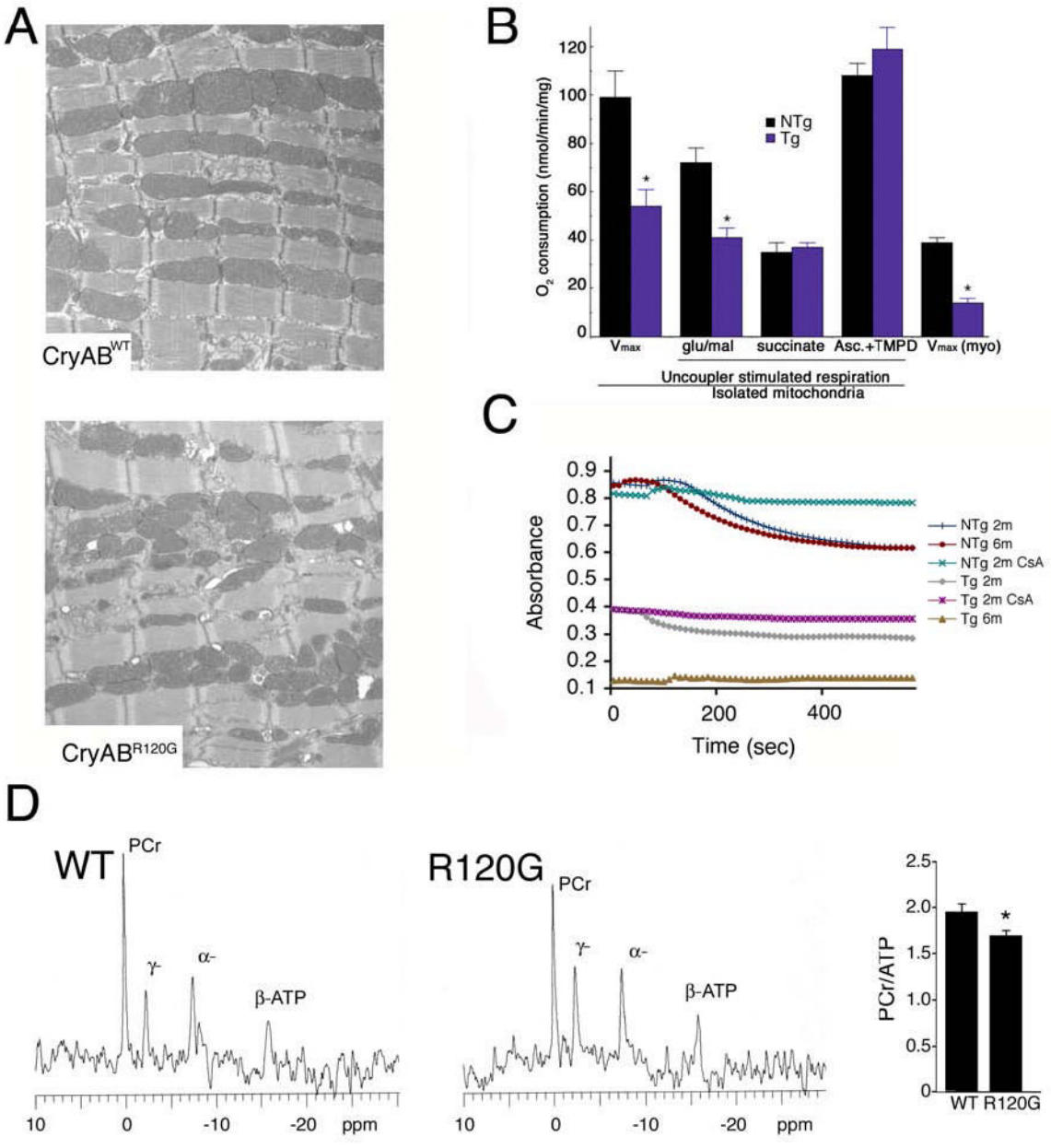

Figure 2.

$CryAB^{R120G}$ expression leads to alterations in cardiac mitochondrial organization and function. A, Shown are electron micrographs derived from 6 week mice expressing equal levels of either $CryAB^{WT}$ or $CryAB^{R120G}$. Note the abnormal architectural relationship of the mitochondria to the sarcomeres in the $CryAB^{R120G}$ cardiomyocytes. B, $CryAB^{R120G}$ mitochondria have impaired respiration at complex I (NADH dehydrogenase complex). The V_{max} for mitochondrial oxygen consumption is significantly reduced in both isolated mitochondria and in situ mitochondria (saponin treated myocytes; myo) derived from $CryAB^{R120G}$ hearts. $n = 3–4$ for isolated mitochondria data and $n = 4–5$ for saponin treated myocytes. $*P < 0.05$ for NTg versus Tg. C, Ca^{2+}-induced swelling in isolated mitochondria. Mitochondria were isolated from the hearts at 2 months or 6 months, primed with 25 mM

NIH-PA Author Manuscript

NIH-PA Author Manuscript

NIH-PA Author Manuscript

Ca^{2+} and swelling induced by the addition of 200 mM $CaCl_2$. (n = 3). D, ^{31}P-NMR spectra were used to evaluate phosphocreatine levels in 8 week $CryAB^{WT}$ and $CryAB^{R120G}$ Langendorff-perfused hearts.

NIH-PA Author Manuscript

NIH-PA Author Manuscript

NIH-PA Author Manuscript

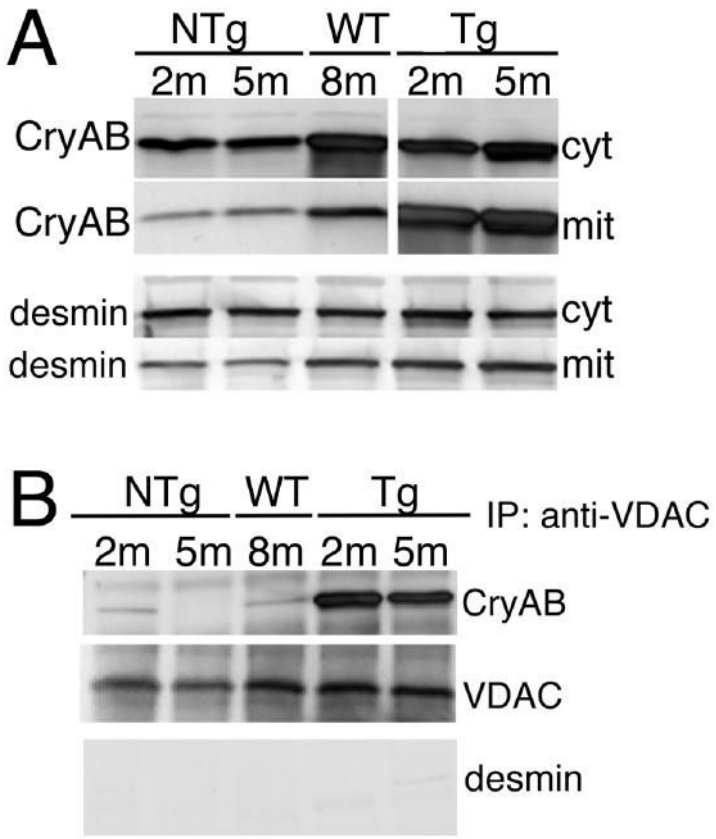

Figure 3.

Association of CryAB with mitochondria A, CryAB levels in mitochondrial (mit) and cytoplasmic (cyt) fractions. The respective fractions were purified from NTg, $CryAB^{WT}$ (WT) or $CryAB^{R120G}$ ventricles, equal amounts of protein loaded onto PAGE gels and CryAB or desmin analyzed via Western blot. B, Co-immunoprecipitation of CryAB with VDAC in mitochondrial fractions. Immunoprecipitated protein was Western blotted with either anti-CryAB and anti-VDAC (to show equivalent inputs). VDAC co-precipitated preferentially with the mutant $CryAB^{R120G}$. The immunoprecipitates were also analyzed for the presence of desmin as a marker for the non-specific association of aggregates with the mitochondria; no significant amounts of desmin were detected. m; month.

NIH-PA Author Manuscript
NIH-PA Author Manuscript
NIH-PA Author Manuscript

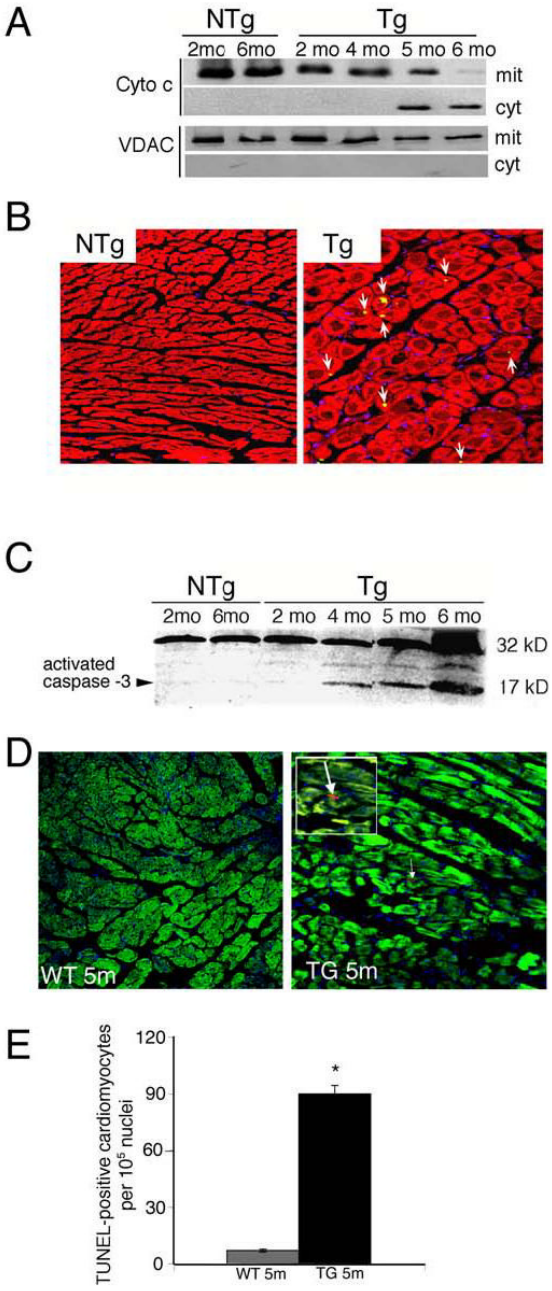

Figure 4.

Apoptotic pathways are activated in CryAB^{R120G} mice. A, Partitioning of cytochrome *c* between the cytosolic and mitochondrial fractions. As the CryAB^{R120G} mice age, cytochrome *c* is released from the mitochondria. The appearance of cytosolic cytochrome *c* was not due to contamination of the fraction with mitochondria, as the mitochondrial protein VDAC was found only in the mitochondrial fraction. B, Immunostaining for activated caspase-3 (appears as yellow) in sections derived from 5 month hearts. Cardiomyocytes were identified by phalloidin staining for actin (red); caspase-3 activity (arrows) is apparent in the CryAB^{R120G} section (Tg). C, Activated caspase-3 levels in ventricular homogenates from NTg (2 and 6 months) and CryAB^{R120G} (Tg) mice (2, 4, 5, 6 months) were detected by Western analysis. D,

NIH-PA Author Manuscript

NIH-PA Author Manuscript

NIH-PA Author Manuscript

TUNEL assays in 5 month hearts derived from $CryAB^{WT}$ and $CryAB^{R120G}$ mice. Cardiomyocytes were identified by phalloidin staining for actin (green). The positive signal was apparent only in the $CryAB^{R120G}$-derived sections and is indicated by an arrow; this region is magnified 3x and shown in the white bordered area. E, Quantitation of TUNEL signal. Between 3–12 × 10^5 nuclei were counted for each sample and the percent TUNEL positive cells determined.

NIH-PA Author Manuscript
NIH-PA Author Manuscript
NIH-PA Author Manuscript

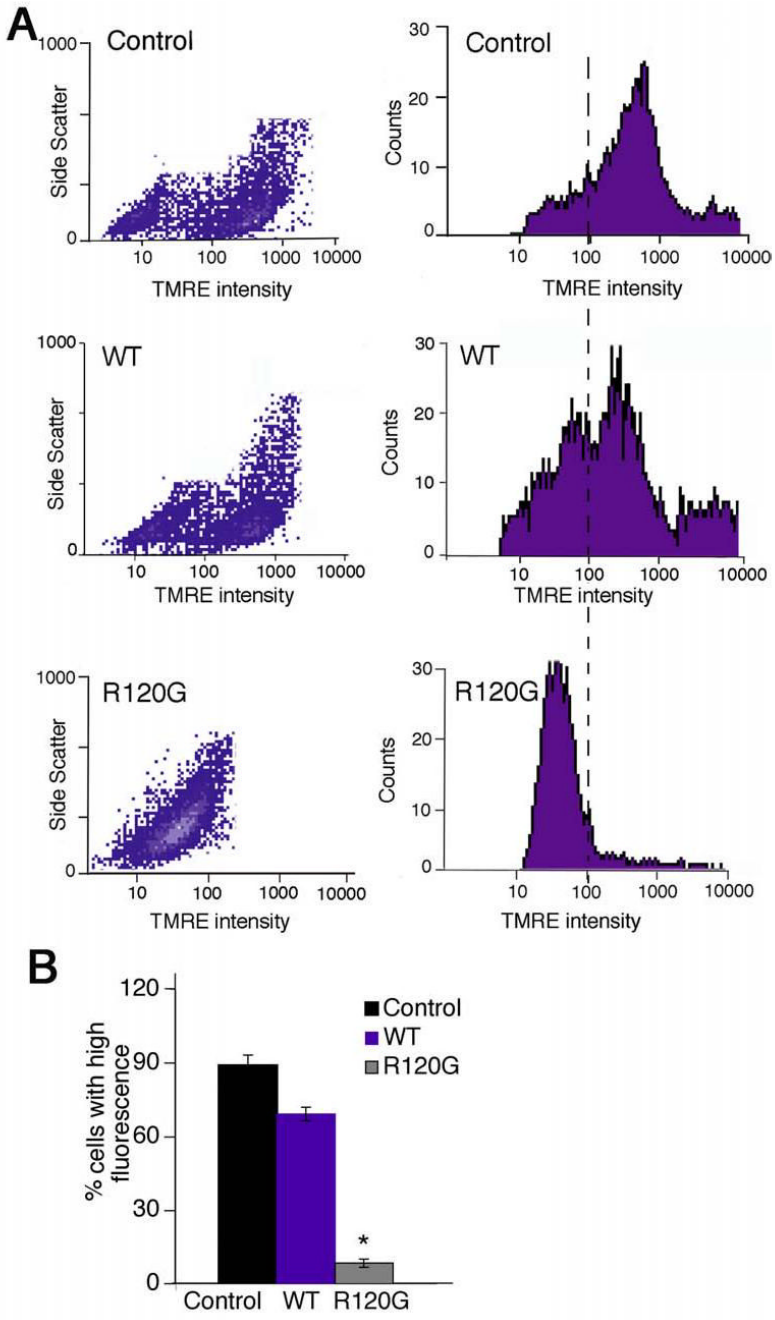

Figure 5.

FACS analysis of TMRE loading in transfected RNC. CryAB^{R120G} expression reduced mitochondrial Δψ as measured by TMRE uptake. A, FL-2 density plots (left) and histograms (right) of FACS data from uninfected cells (control), RNC transfected with adenovirus containing CryAB^{WT} (WT) or adenovirus containing CryAB^{R120G}. MOI's were 10 and resulted in equal levels of normal or mutant CryAB expression that approximated the level of overexpression observed in the CryAB^{R120G} model previously reported.[5] Cardiomyocytes were loaded by treatment with 50 nM TMRE. CryAB^{R120G} expression decreased TMRE fluorescence and shifted the distribution curve leftward, indicating Δψ depolarization. B, TMRE fluorescence was determined from 3 independent experiments and the percentage of

cells falling to the right of an arbitrary threshold of 100 (dotted line) is shown. Approximately 20,000 cells were included in each experiment, which was done in duplicate. *$P < 0.0001$ versus Control

NIH-PA Author Manuscript
NIH-PA Author Manuscript
NIH-PA Author Manuscript

NIH-PA Author Manuscript

NIH-PA Author Manuscript

NIH-PA Author Manuscript

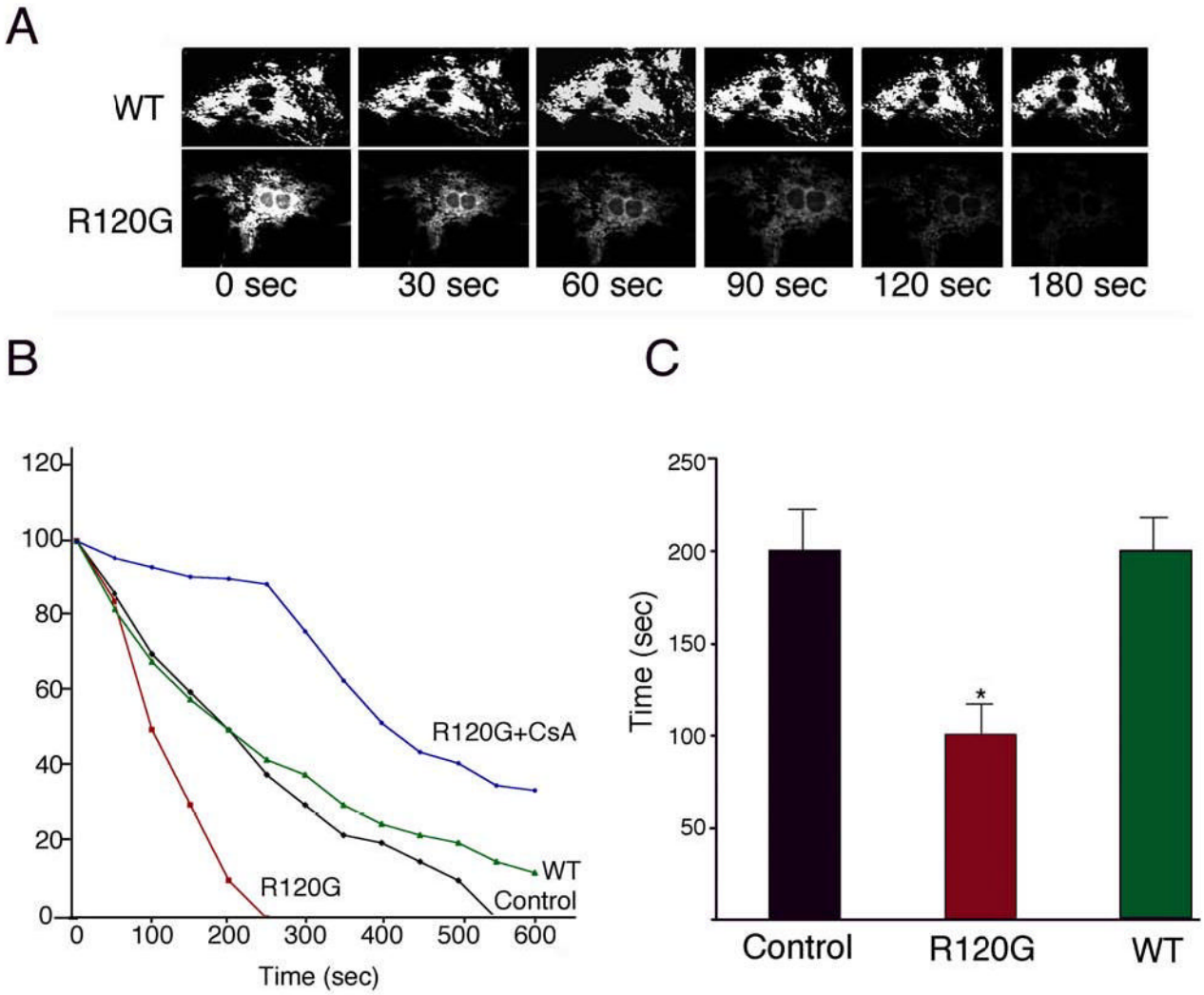

Figure 6.

Time lapse analysis of Δψ loss. RNC were transfected as in Figure 5. Five days post-infection, cells were loaded with TMRE, treated with 100 nM of the uncoupler CCCP and time lapse confocal microscopy begun. A, Sequential images for TMRE intensity for each group. B, Time course of normalized TMRE intensity. The average TMRE brightness from ≥ 30 myocytes from each plate was collected at the indicated times. To confirm the PTP-dependency of the onset of TMRE loss, transfected cardiomyocytes were treated with CsA prior to exposure to CCCP. CsA significantly delayed Δψ dissipation. C, Time to 50% loss of TMRE intensity. (**P* < 0.05 versus Control or WT)

NIH-PA Author Manuscript

NIH-PA Author Manuscript

NIH-PA Author Manuscript

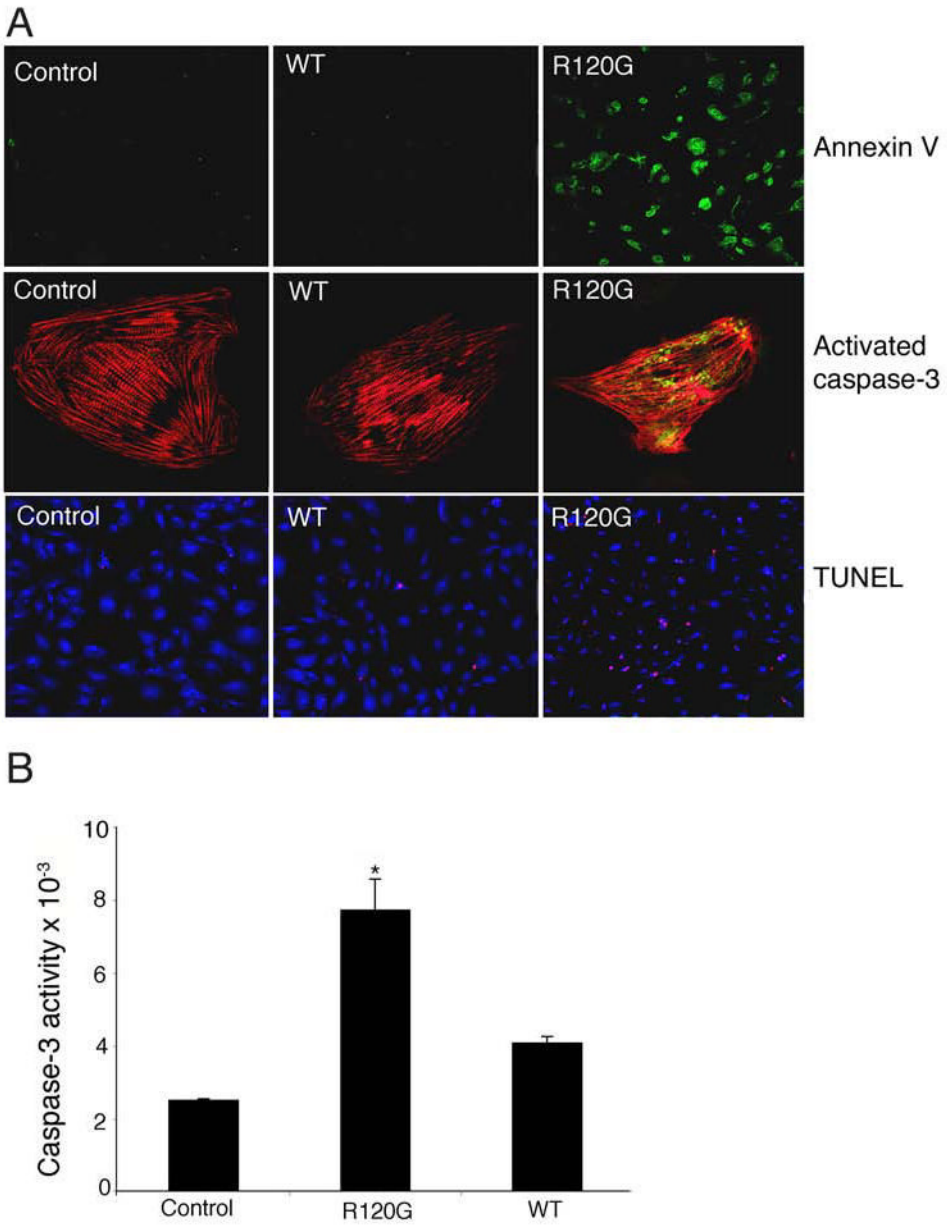

Figure 7.

R120G expression activates apoptotic processes in RNC. A, Cells were either untreated (Control), or transfected with adenovirus containing normal CryAB^{WT} (WT) or adenovirus encoding CRYAB^{R120G} (R120G). Apoptotic markers were detected by immunofluorescence 5 days post-infection. Cardiomyocytes were identified by TnI (red). B, Caspase-3 activity in homogenates prepared from the cultures. $P < 0.001$ for CRYAB^{R120G} versus CRYAB^{WT}-transfected cells.